

EVALUATION OF PREVIEW G-VECTORING CONTROL TO DECELERATE A VEHICLE PRIOR TO ENTRY INTO A CURVE

J. TAKAHASHI^{1)*}, M. YAMAKADO²⁾ and S. SAITO³⁾

¹⁾Transportation, Energy & Environment Research Laboratory, Hitachi Europe GmbH, Lohstrasse 28, Schwaig-Oberding, Germany

²⁾Hitachi Research Laboratory, Hitachi, Ltd., 832-2 Horiguchi, Hitachinaka, Ibaraki, Japan

³⁾Hitachi Construction Machinery Co., Ltd., 650 Kandatsumachi, Tsuchiura, Ibaraki, Japan

(Received 7 January 2013; Revised 2 March 2013; Accepted 5 March 2013)

ABSTRACT—This paper describes the development of the braking assistance system based on a “G-Vectoring” concept. The present work focuses in particular on “Preview G-Vectoring Control” (PGVC), which is based on the “G-Vectoring Control” (GVC) scheme. In GVC, the longitudinal-acceleration control algorithm is based on the actual lateral jerk. PGVC decelerates a vehicle before it enters a curve, and is based on a new longitudinal-acceleration control algorithm which uses predicted and actual lateral jerk. Using the predicted lateral jerk makes it possible to decelerate the vehicle prior to curve entry. This deceleration can emulate a driver’s deceleration as the vehicle approaches a curve entry. PGVC is based on such deceleration algorithms and enables automatic deceleration similar to the action of a driver. It is thus possible to significantly improve the driver’s feeling when this system is activated. Driving tests with this new control system on snowy-winding course confirmed that the automatic brake control quality improved considerably compared to manual driver control considering both lap time and ride quality. These results indicate that PGVC can be a useful braking assistance system not only to improve the driver’s handling performance but also to reduce the brake-task during driving on winding roads.

KEY WORDS : Vehicle dynamics, Driver assistance system, Chassis system

1. INTRODUCTION

Fuel consumption during driving strongly depends on the driver’s acceleration/deceleration: indeed, constant-speed drive would improve the fuel efficiency. However, there are many factors to influence the deceleration on the road (other vehicles, signal, course curvature etc.), and the driver has to control the acceleration/ deceleration depending on the situation.

In particular, the fuel consumption during cornering strongly depends on the driver’s skill; some unskilled drivers run excessive deceleration and acceleration, and such driving style increases the fuel consumption and sometimes may cause accidents, especially on a slippery surface. Even for the skilled driver, it may be hard to control acceleration/deceleration on slippery winding roads. To reduce the driver’s pedal work during driving on a winding road, it is useful to implement the “G-Vectoring Control” (GVC), based on Equation (1), as follows:

$$G_{xt_GVC} = -sgn(G_y \cdot \dot{G}_y) \frac{C_{xy}}{1+T_S} |\dot{G}_y| \quad (1)$$

With GVC, the longitudinal-acceleration command G_{xt_GVC} is given as a value assigned first-order delay by multiplying the lateral jerk (first derivative of acceleration) acting on a vehicle (G_y) by the gain C_{xy} . It was confirmed that GVC can improve the vehicle motion from the viewpoint of both handling and ride quality (Yamakado *et al.*, 2010; Takahashi *et al.*, 2012). However, many drivers desire deceleration prior to entry into a tight curve; it is necessary to control longitudinal-acceleration before lateral-acceleration increases.

In the present study, a new longitudinal-acceleration control technique named Preview G-Vectoring Control (PGVC) was investigated. PGVC can decelerate the vehicle prior to entry into a curve using curvature data of the road ahead (see Figure 1).

In our previous paper (Takahashi *et al.*, 2011), it was confirmed that the deceleration calculated by this algorithm can simulate the driver’s deceleration before the vehicle enters into a curve. In this paper, PGVC is developed and evaluated by actual driving tests on a snowy-winding course.

2. DEVELOPMENT OF PREVIEW G-VECTORING CONTROL

2.1. Basic Pre-cornering Deceleration Model

*Corresponding author. e-mail: junya.takahashi.kd@hitachi.com

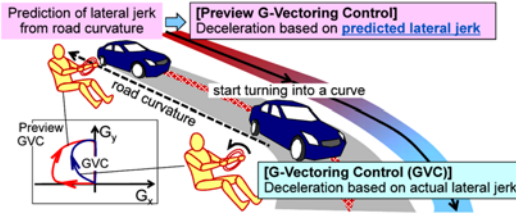


Figure 1. Preview G-Vectoring concept.

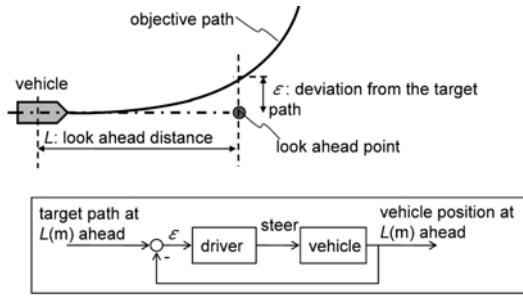


Figure 2. Driver model of steering.

In regard to steering in response to the shape of the course, a driver model has been proposed (see Figure 2) (Kondo and Ajimine, 1968; Abe, 2009). This driver model—called a “look-ahead” model—takes into consideration the simplest steering control by a driver. As shown in Figure 2, a point at distance L in front of the vehicle (hereafter, look-ahead point) is set, and the deviation of the target path from the look-ahead point (ε) is fed back, and steering is executed accordingly. Taking the curve entry time into consideration, this model will give the condition under which steering starts before the vehicle enters the curve.

As for acceleration/deceleration actions, it is conceivable that the driver visually confirms the shape of the course ahead and executes acceleration or deceleration in accordance with that perception. Generally speaking, the look-ahead model in regard to steering is analogous with prior-curve deceleration action. Here, this general concept (namely, look-ahead) is used, and the acceleration/deceleration model is studied. Figure 3 shows the longitudinal-acceleration model based on a general look-ahead concept using a preview point (a point on the course ahead of the vehicle by distance L_{pv}): the velocity of this point (V_{pv}), vehicle velocity (V), and road-curvature at the preview point

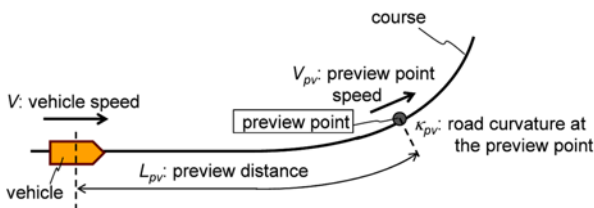


Figure 3. Definition of preview point.

(κ_{pv}). When the vehicle is traveling at constant velocity V at the preview point, lateral-acceleration generated on the vehicle ($G_{y,pv}$) is given in Equation (2) as follows.

$$G_{y,pv} = \kappa_{pv} \cdot V^2 \tag{2}$$

By assuming that acceleration/deceleration is executed with an equivalent algorithm to longitudinal-acceleration control in response to lateral motion of the vehicle (i.e., GVC), it is possible to control longitudinal-acceleration before lateral motion of the vehicle actually occurs. With GVC, on the basis of the above-mentioned assumption, longitudinal-accelerations corresponding to $G_{y,pv}$ are calculated by using $G_{y,pv}$ in place of the lateral jerk (G_y) given by Equation (1). In this manner, a longitudinal-acceleration command value ($G_{xt,pv}$) related to the lateral motion of the vehicle that will be generated (not lateral motion of the vehicle that is generated) is given. Under the some assumptions (κ_{pv} is positive, V is constant), $G_{xt,pv}$ is given by Equation (3) from Equations (1), (2) using gain ($C_{xy,pv}$) and time constant (T_{pv}).

$$G_{xt,pv} = -\frac{C_{xy,pv}}{1 + T_{pv}s} \cdot \dot{\kappa}_{pv} \cdot V^2 \tag{3}$$

According to Equation (3), $G_{xt,pv}$ takes a form that is proportional to $\dot{\kappa}_{pv}$, and it can be said to give a new acceleration/deceleration model that takes into account the course shape ahead of the vehicle. In this study, the deceleration part of this model is focused as a pre-coringer deceleration model.

Driving tests were performed on the R40 steering course (see Figure 4) to compare $G_{xt,pv}$ with the driver’s deceleration behavior near the curve entry. The tests imposed the two tasks outlined below.

- (a) Transit speed at point P in is assumed to be set at the initial speed V_0 .
- (b) After point P, acceleration and deceleration are performed as required to trace the target path.

For calculating longitudinal-acceleration command values ($G_{xt,pv}$), the layout data of the R40 steering course (shown in Figure 4) is acquired a priori, and the created map data (longitude, latitude and road-curvature at 5 m node resolution) are used. Figure 5 shows the road-curvature at each node along the R40 steering course. In this figure, the node number at point P shown in Figure 4 is

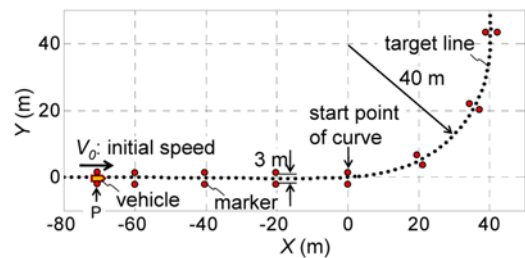


Figure 4. Layout of R40 steering course.

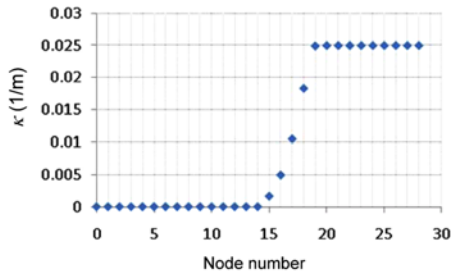


Figure 5. Node number and road-curvature of R40 steering course.

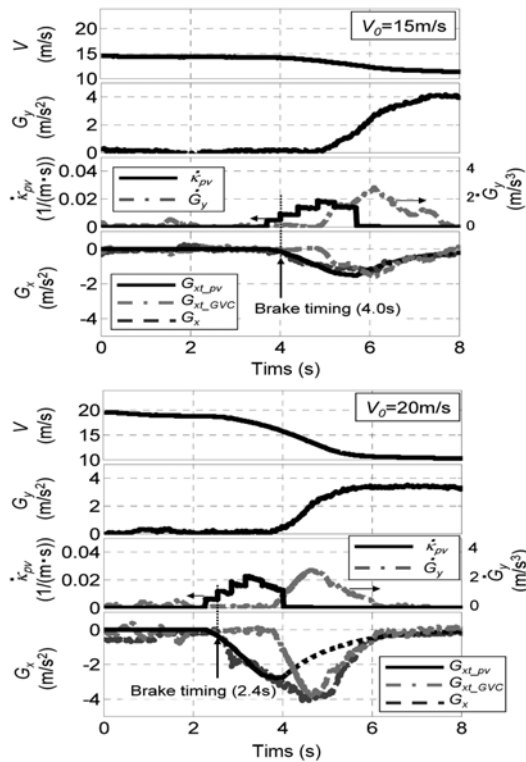


Figure 6. Comparison of longitudinal-acceleration caused by driver's braking and calculation result of Equation (3) ($V_0 = 15 \text{ m/s}, 20 \text{ m/s}$).

denoted as zero.

Figure 6 shows the results at 15 m/s and 20 m/s as initial speed (V_0). In these figures, G_{xt_pv} (solid line) is calculated using Equation (3) and G_{xt_GVC} (dashed-dotted line) is calculated using Equation (1). Here, L_{pv} is given as the product of velocity V and look-ahead time t_{pv} to accomplish the driver's action; looking further ahead at high velocity. In these cases, t_{pv} is set at 2.1 s.

As clear from Equation (3), under these conditions, deceleration occurs before generation of lateral acceleration; the driver executes deceleration control before entering the curve, and the generated deceleration increases as set velocity increases. As shown in these figures, time variation of road-curvature at the preview point ($\dot{\kappa}_{pv}$)

increases before lateral acceleration increases (namely, before curve entry), and the time at which that increase starts and the time starts to increase deceleration take similar values (4.0 s at V_0 of 15 m/s and 2.4 s at 20 m/s).

Furthermore, as set velocity increases, $\dot{\kappa}_{pv}$ takes a bigger value, and G_{xt_pv} take a form similar to longitudinal-acceleration generated by the driver (G_x) before generation of lateral-acceleration (G_y). After G_y starts increasing, it is possible to simulate G_x by G_{xt_GVC} . By combining both, deceleration actions from curve entry to steady-state steering could be re-created.

2.2. Extended Pre-cornering Deceleration Model

The application of the pre-cornering deceleration model to PGVC, G_{xt_pv} should be adapted to the driver's deceleration not only near but also far from the curve. However, G_{xt_pv} cannot be the same trend with the driver's deceleration in the case the driver starts braking while still far from the curve.

Figure 7 shows the comparison of longitudinal-acceleration caused by driver's braking and calculated result of Equation (3) at V_0 of 24 m/s. In the case, t_{pv} of 2.1 s (same value with Figure 6), $\dot{\kappa}_{pv}$ increases before lateral acceleration G_y increases (see Figure 7A), and G_{xt_pv} is almost same value with the driver's deceleration (see Figure 7B). However, deceleration timing of G_{xt_pv} is too late compared to the driver's one (see Figure 7C). This difference is caused by the timing delay when the preview point reaches the curve.

To make this timing earlier, it is necessary to extend L_{pv} ; that is, t_{pv} is set to a bigger value. As shown in Figure 7D, if t_{pv} is set at 3.2 s, it is possible to make the deceleration-start timing of G_{xt_pv} almost same as the driver's one. However, the trend of G_{xt_pv} is quite different from the one caused by the driver's braking (see Figure 7E); there is a too much deceleration caused by G_{xt_pv} at the beginning of deceleration.

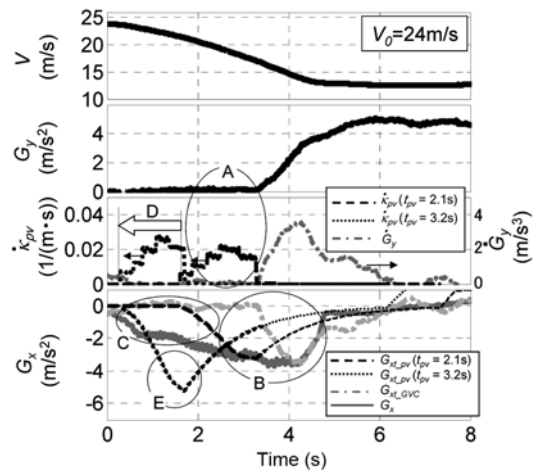


Figure 7. Comparison of longitudinal-acceleration caused by driver's braking and calculation result of Equation (3) ($V_0 = 24 \text{ m/s}$).

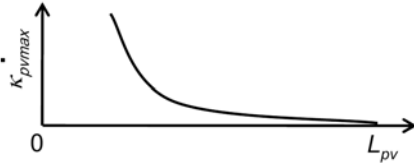


Figure 8. Relationship between L_{pv} and $\dot{\kappa}_{pvmax}$.

tion. This result indicates that the pre-cornering deceleration model described by Equation (3) does not work well when the brake-start point is relatively far from the curve.

The pre-cornering deceleration model described by Equation (3) is based on the assumption that a driver decelerates the vehicle using the curvature information ($\dot{\kappa}_{pv}$). As shown in , G_{xt_pv} calculated by Equation (3) could simulate the driver's deceleration when the vehicle position is close to the curve; that is, this assumption would work well in this case. However, if the vehicle is far from the curve, it would be hard for a driver to get detailed information of curvature (such as $\dot{\kappa}_{pv}$), even though the driver could perceive the curve. In this case, the driver would not use $\dot{\kappa}_{pv}$ to decelerate the vehicle; that is, the assumption that a driver decelerates the vehicle using $\dot{\kappa}_{pv}$ does not work and G_{xt_pv} could not simulate the driver's deceleration.

To adapt G_{xt_pv} to the driver's deceleration even though the vehicle position is far from the curve, $\dot{\kappa}_{pv}$ is limited using the upper limit ($\dot{\kappa}_{pvmax}$) as shown in Figure 8. This limitation is set from the viewpoint of the driver's visual-information-limit; as L_{pv} becomes larger, $\dot{\kappa}_{pvmax}$ becomes quite smaller. This limitation affects V_{pv} because of the relationship between $\dot{\kappa}_{pv}$ and V_{pv} , as shown in Equation (4).

$$\dot{\kappa}_{pv} = \frac{dx}{dt} \cdot \frac{d\dot{\kappa}_{pv}}{dx} = V_{pv} \cdot \frac{d\dot{\kappa}_{pv}}{dx} \quad (4)$$

Here, the preview point speed without limitation (V_{pv0}) is given by Equation (5) using look-ahead time (t_{pv}), longitudinal-acceleration (G_x) and V . Furthermore, L_{pv} is given by the integration of the relative speed ($V_{pv} - V$).

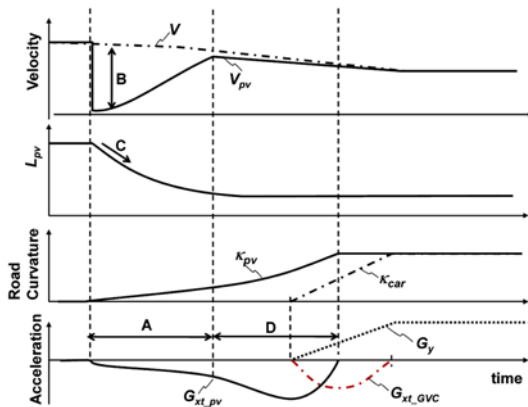


Figure 9. Relationship between V_{pv} , L_{pv} , κ_{pv} and G_{xt_pv} .

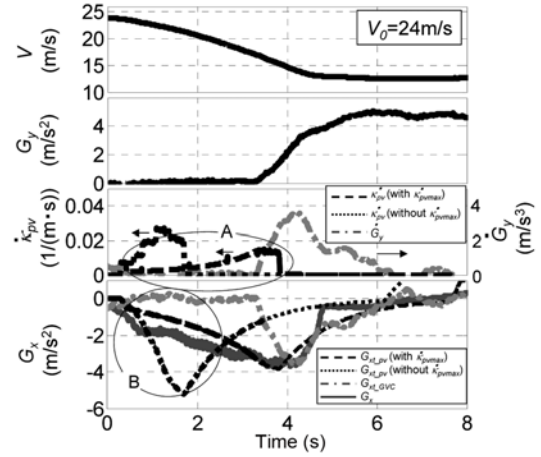


Figure 10. Comparison of longitudinal acceleration caused by driver's braking and calculation result of Equation (3) using $\dot{\kappa}_{pvmax}$ ($V_0 = 24$ m/s).

$$V_{pv0} = t_{pv} \cdot G_x + V \quad (5)$$

When L_{pv} is quite large, $\dot{\kappa}_{pv}$ is limited by $\dot{\kappa}_{pvmax}$ and G_{xt_pv} would be small (see Figure 9A). As shown in Equation (4), if $d\dot{\kappa}_{pv}/dx$ is not zero, V_{pv} is also limited by $\dot{\kappa}_{pvmax}$ and would become smaller than V (see Figure 9B). As a result, L_{pv} would decrease gradually (see Figure 9C), because the relative speed ($V_{pv} - V$) would be negative. This decrease of L_{pv} would cause the increase of $\dot{\kappa}_{pvmax}$ (i.e., $\dot{\kappa}_{pv}$); the G_{xt_pv} limited by $\dot{\kappa}_{pvmax}$ would increase as the vehicle closes to the curve (see Figure 9D).

Figure 10 shows the test result shown in and the recalculated result of G_{xt_pv} with $\dot{\kappa}_{pvmax}$. As shown in A, $\dot{\kappa}_{pv}$ with $\dot{\kappa}_{pvmax}$ is smaller than the one without $\dot{\kappa}_{pvmax}$ at the beginning of increase, and it increases gradually close to the time when lateral-acceleration (G_y) increases; $\dot{\kappa}_{pv}$ is strongly limited by $\dot{\kappa}_{pvmax}$ at the beginning, and this value increases as the vehicle approaches to the curve. This limitation could prevent the rapid deceleration like the G_{xt_pv} without $\dot{\kappa}_{pvmax}$ (dashed line) as shown in B. As a result, G_{xt_pv} with $\dot{\kappa}_{pvmax}$ (broken line) increase gradually while approaching the curve, and it takes a form similar to the driver's deceleration (G_x ; solid line).

This result indicates that the pre-cornering deceleration model could be extended to simulate the driver's deceleration even if the vehicle position is far from the curve. PGVC was developed based on this extended pre-cornering deceleration model with gain control, filtering to combine G_{xt_pv} and G_{xt_GVC} smoothly and dead zone.

3. EVALUATION OF PREVIEW G-VECTORIZING CONTROL BY DRIVING TESTS

3.1. Outline of the Driving Tests

Figure 11 shows the outline of the test vehicle and Figure

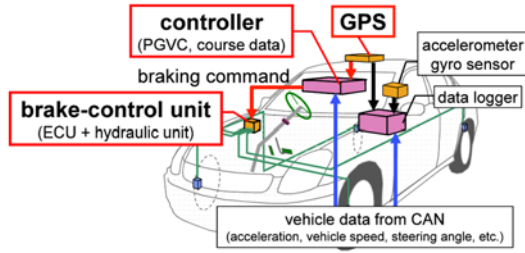


Figure 11. Outline of the test vehicle.

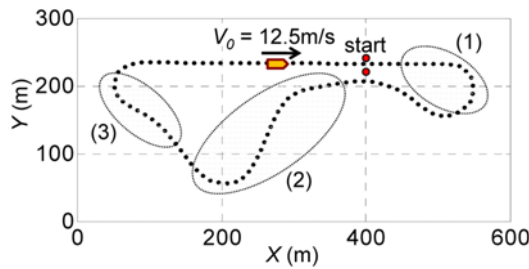


Figure 12. Outline of the course layout.

12 shows the course layout. The test vehicle is additionally equipped with a controller and a GPS (frequency: 20 Hz; distance-measurement accuracy: 0.5 m). The controller acquires the signals from the GPS and a controller area network (CAN). PGVC logic and the curvature data of the course are implemented in the controller and the brake-control unit decelerates the vehicle via the braking command from the controller. Lateral-acceleration and longitudinal-acceleration are measured by an acceleration sensor (frequency: 100 Hz; resolution: 0.006 m/s²).

Driving tests were performed by the three drivers (A, B, C) who got trained to drive in our proving ground and have a certain level of driving skill, each of whom completed the course (see Figure 12) three times with and without PGVC. All tests were performed on a snowy surface. The requested tasks for the driver are as follows:

- (a) Drive as fast as possible with following the course
- (b) Upper limit of the speed is 12.5 m/s

The performance of PGVC was evaluated at the section (1) to (3) (shown in Figure 12) by comparison of the results with and without PGVC. The integral of the square jerk ($\dot{G}_x^2 + \dot{G}_y^2$) (named “Index J”) and the transit time of each section (named “Index T”) were used as evaluation indices: small values of these indices imply low energy loss, a good ride quality and high transport efficiency.

3.2. Results of the Driving Tests

Figure 13 shows the results of the driving tests with and without PGVC at section (1) by driver A: steering angle (*str*), vehicle speed (*V*), longitudinal-acceleration (G_x) and lateral-acceleration (G_y). In (a), without PGVC case, G_x and G_y (that is, acceleration/deceleration and steering angle)

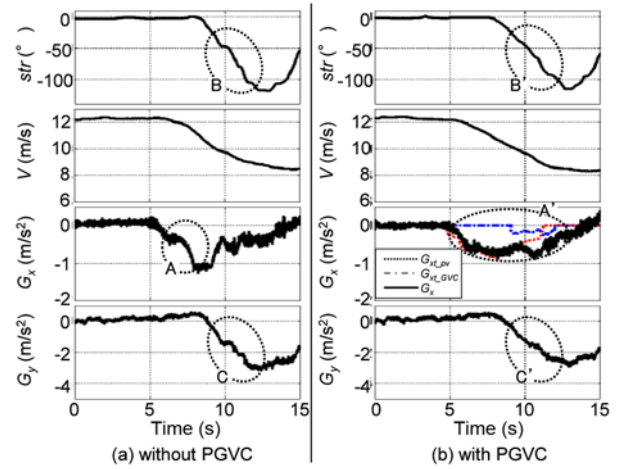


Figure 13. Driving test results (Section (1), driver A).

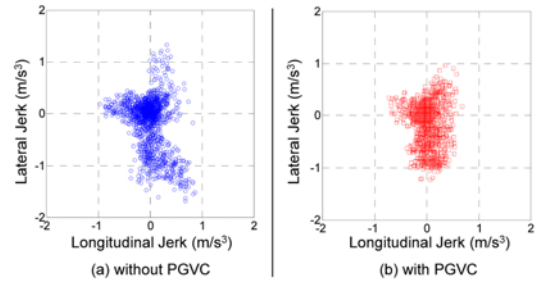


Figure 14. Longitudinal and lateral jerk with or without PGVC (Section (1), driver A).

were controlled by driver himself, and in (b), with PGVC case, only deceleration was controlled automatically by PGVC.

As shown in Figure 13A', G_x caused by G_{x_pv} (dotted line) and G_{x_GVC} (dashed-dotted line) changes smoothly, as compared to G_x caused by driver’s braking (see Figure 13A). In addition, the increase of steering angle in (b) with PGVC case also becomes smoother than that in (a) without PGVC case (see Figure 13B, B’), even though PGVC controlled only deceleration. As the result, in (b) with PGVC case, both G_x and G_y change smoothly (see Figure 13C, C’).

To see the smoothness of acceleration clearly, the longitudinal and lateral jerk (\dot{G}_x, \dot{G}_y) are plotted. Figure 14 shows the longitudinal and lateral jerk (\dot{G}_x, \dot{G}_y) with and without PGVC at section (1) by driver A.

In (b), with PGVC case, the absolute-maximum values of both \dot{G}_x and \dot{G}_y are smaller than that of (a) without PGVC case. As mentioned above, PGVC generated only deceleration in these tests, and the other motions (such as speed-up, turning) are controlled by the driver. However, PGVC affects the driver’s steering and accelerator-pedal behavior, and reduces not only \dot{G}_x (controlled by PGVC directly) but also \dot{G}_y (controlled by the driver himself).

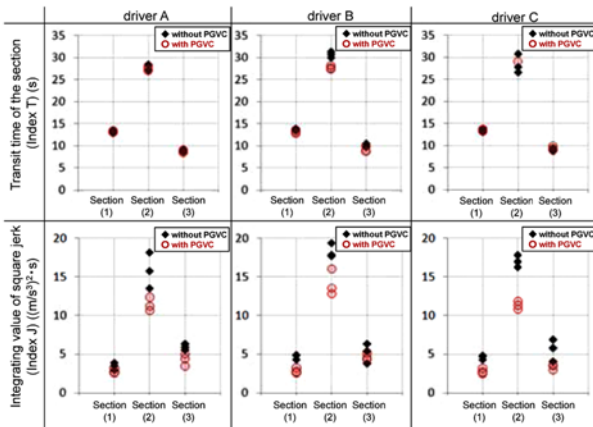


Figure 15. Transit time of the each section and integrating value of square jerk.

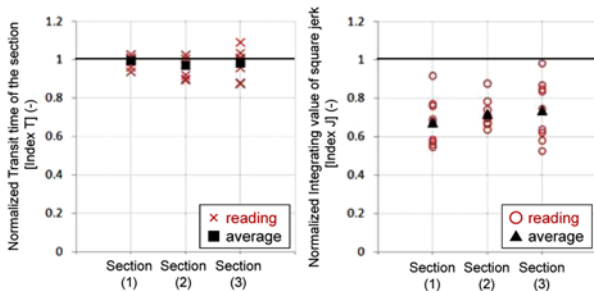


Figure 16. Transit time of the each section and integrating value of square jerk (normalized).

In (a), without PGVC case, the driver had to handle the steering-wheel while controlling the brake-pedal on the snowy road. On the other hand, in (b), with PGVC case, PGVC generated the deceleration prior to entry into a curve, and it freed the driver from the combined task of steering and braking. As a result, the driver could concentrate on the steering task, and his control performance would be improved. This point could be noted in the driver’s comment that the deceleration of PGVC made the driving tasks easy, even on the slippery surface.

Figure 15 shows the test results of Index T (the transit time of each section) and Index J (the integral of the square jerk) of the three drivers. Index T and Index J are different for the drivers, even though they drove the same course. However, in each case, PGVC could reduce Index J even though Index T is almost the same. To clarify these tendencies, each driver’s result (Index T, Index J) with PGVC were normalized by the one without PGVC.

Figure 16 shows the normalized Index T and Index J.

The average of normalized Index J is obviously smaller than 1 in each section, even though the average of normalized Index T is almost 1 or smaller; PGVC could reduce the jerk significantly without the excessive slow-down.

These results indicate that PGVC could improve the energy loss and ride quality with no degradation in transport efficiency during the driving on the winding, snowy road. Moreover, every driver commented that the vehicle was decelerated automatically as they expected and they could concentrate on the steering and accelerator-pedal operation. According to the results above, PGVC could be a useful driver assistance system to reduce the driver’s brake task, especially on slippery surfaces.

4. CONCLUSION

A new longitudinal-acceleration control named Preview G-Vectoring Control (PGVC), which controls longitudinal motion by predicted and actual lateral motion of the vehicle, was developed and evaluated by driving tests on a snowy road. The test results are summarized as follows: first, the pre-cornering deceleration model based on the G-Vectoring concept is extended to simulate the driver’s deceleration even if the vehicle position is far from the curve. Secondly, it was confirmed that PGVC based on this model could reduce the jerk without excessive slow-down. For these reasons, it can be concluded that PGVC could be a useful driver assistance system to reduce the driver’s braking task.

REFERENCES

Abe, M. (2009). *Vehicle Handling Dynamics*. Butterworth - Heinemann.

Kondo, M. and Ajimine, A. (1968). Driver’s sight point and dynamics of the driver-vehicle system related to it. *Proc. SAE Automotive Engineering Cong.*, Detroit, MI.

Takahashi, J., Yamakado, M. and Saito, S. (2011). A Study on an Acceleration/Deceleration Model Based on Time Variation of Road Curvature Ahead of a Running Vehicle. *FAST-Zero’11*.

Takahashi, J., Yamakado, M., Saito, S. and Yokoyama, A. (2012). A hybrid stability-control system: combining direct-yaw-moment control and G-vectoring control. *Vehicle System Dynamics* **50**, 6, 847–859.

Yamakado, M., Takahashi, J., Saito, S., Yokoyama, A. and Abe, M. (2010). Improvement in vehicle agility and stability by G-vectoring control. *Vehicle System Dynamics*, **48**, 231–254.